Eur J Cancer Clin Oncol, Vol. 23, No. 9, pp. 1385–1390, 1987.
Printed in Great Britain

0277–5379/87$3.00+0.00

Methotrexate and 7-Hydroxy-methotrexate Pharmacokinetics Following Intravenous Bolus Administration and High-dose Infusion of Methotrexate*

PATRICK BORE,† RENE BRUNO,†‖ NICOLE LENA,‡ ROGER FAVRE‡ and JEAN PAUL CANO†§

†*INSERM U* 278, *Faculté de Pharmacie*, 27, *bd Jean Moulin*, 13385 *Marseille cédex* 5, *France and* ‡*Institut Paoli Calmettes*, 232 *Bd de Sainte Marguerite*, 13273 *Marseille Cedex* 9, *France*

Abstract—*The pharmacokinetics of methotrexate and 7-hydroxy-methotrexate were studied in patients undergoing very high-dose methotrexate monotherapy. The patients received, first, two methotrexate intravenous bolus test doses* (50 mg/m^2) *one with and one without concomitant administration of folinic acid* (15 mg *every* 6 h) *in a random sequence, and, second, an* 8 h *infusion, individualized to achieve a peak plasma concentration of* 5×10^{-4} M *methotrexate* (*infusion rates* > 1000 mg/h). *Methotrexate and 7-hydroxy-methotrexate concentrations were measured by specific radioimmunoassays and the data were analysed simultaneously by an integrated pharmacokinetic model. Following test dose administration, methotrexate and 7-hydroxy-methotrexate plasma concentration kinetics were best described by assuming that methotrexate elimination (and 7-hydroxy-methotrexate formation) occurred from a peripheral compartment reaching rapid equilibrium with the plasma. Folinic acid administration did not influence the disposition of either compound. Following the infusion, a significant* ($P < 0.01$) *decrease of methotrexate total plasmatic clearance occurred without modification of 7-hydroxy-methotrexate formation and elimination.*

INTRODUCTION

IDENTIFICATION of methotrexate (MTX) pharmacokinetics and plasma level monitoring are very useful in providing guidelines for high-dose MTX infusions (HDI) and especially in optimizing the infusion rate, both of which are destined to prevent toxic side-effects and to adjust the folinic acid (FA) rescue [1–6]. Pharmacokinetic approaches using simple linear compartment models have been found to perform well in predicting steady-state levels achieved following a wide range of MTX infusion rates (17–650 mg/h) [3, 5, 6] and, to a certain extent, MTX kinetics following infusion [5]. However, limitations in predictive capabilities were observed both during FA rescue [5] and in the case of very high infusion rates (> 970 mg/h) [6]. FA rescue is known to interfere with MTX transport at the cellular level [7]; however, the influence of FA on MTX kinetic behaviour has not yet been studied.

7-Hydroxy-methotrexate (OH-MTX), the major circulating metabolite of MTX, is an important determinant of MTX toxicity [1] and even activity [8, 9]. This metabolite has been found in relatively high plasma concentrations in patients [10–13]. Moreover metabolic saturation during very high MTX infusion rates (> 970 mg/h) might contribute to the lack of reliability in predicting MTX levels. Therefore OH-MTX kinetics should be taken into account when studying MTX phamacokinetics.

In this paper we assess MTX and OH-MTX pharmacokinetics following (i) intravenous bolus of MTX with and without concomitant administration of FA and (ii) the subsequent individualized high-dose infusion in order to study influences of both FA administration and very high-dose infusion rates on MTX disposition and metabolism.

Accepted 11 May 1987.
*This work was supported by a grant from the Comité Départemental des Bouches-du Rhône de la Ligue Nationale Française contre le Cancer and by Institutional grants from INSERM.
‖Present address: Recherche Syntex France, Leuville-Sur-Orge, BP 40, 91310 Montlhery, France.
§To whom requests for reprints should be addressed.

Table 1. Patient characteristics

Patient	Age/ weight	Serum creatinine (μmol/l)	Sex	Diagnosis		Concomitant medication
1	67/60	86	M	Head and neck cancer		None
2	25/55	70	M	Soft tissue sarcoma (hand)	Lung metastasis	None
3	65/75	87	F	Thymic carcinoma	Lung metastasis	Heparin, calcium salt (Calciparine®)
4	17/72	62	M	Osteosarcoma (femur)	Lung metastasis	None
5	33/54	55	M	Soft tissue sarcoma (foot)	Lung metastasis	None
6	27/56	64	M	Osteosarcoma (humerus)	Lung metastasis	None
7	46/49	48	M	Soft tissue sarcoma (leg)	Lung metastasis	Ethylbiscoumacetate (Tromexane®)
8	41/70	181	M	Testicular carcinoma	Lung metastasis	None

MATERIALS AND METHODS

Patients

Eight patients (seven men, one woman) with various neoplastic diseases treated with individualized high-dose MTX monochemotherapy participated in the study after giving informed consent. Patient data are listed in Table 1. Liver and renal functions were within the normal range for all patients at the time of the study, except patient No. 8 who had slightly increased serum creatinine.

Protocol

MTX HDI was individualized after identification of the pharmacokinetic parameters for each patient on the basis of plasma concentrations measured after administration of a small test-dose (TD) intravenous bolus (50 mg/m^2) [3, 6]. This test-dose protocol is a standardized procedure in high-dose MTX therapy in our institution. Patients received another 50 mg/m^2 TD associated with an FA injection (TD-FA) of 15 mg, 1 h after MTX bolus and then every 6 h for 48 h. TD and TD-FA administrations were given 1 week apart in a random sequence to seven out of eight patients (see Table 2). The first HDI, individualized to achieve a 5×10^{-4} M plasma MTX concentration at 8 h [3, 6] was administered at least 1 week following the last intravenous bolus to seven patients. The dose ranged between 1142 and 2186 mg/h for patients Nos. 2–7 and was 485 mg/h for patient No. 8. Complete information about the protocol especially concerning therapeutic monitoring hydration, urine alkalinization and folinic acid rescue has been previously reported [3, 14].

The sampling protocol was the following: time 0 (predrug), 0.25, 0.5, 1, 3, 4, 6, 12, 24, 30, 36 and 48 h following TD and TD-FA administration and time 0 (predrug) 5, 8 (end of infusion), 9, 10, 12, 14, 24, 30, 36, 40, 48, 54, 60, 72, 80, 92 and 116 h following HDI. Venous blood (5 ml) was drawn into heparinized tubes. Plasma samples were collected and stored frozen at −30°C until analysis.

Sample assay

Plasma samples were assayed for MTX and OH-MTX by specific radioimmunoassays (RIA). Coefficients of variation for duplicate determinations were less than 15% between 0.06 and 1.2 nmol/l for MTX and between 0.08 and 9 nmol/l for OH/MTX. The cross reactivity factors were 2.5×10^{-4} and 5×10^{-5}, respectively, for MTX in OH-MTX RIA and for OH-MTX in MTX RIA. In addition, results obtained by RIA and by high performance liquid chromatography were well correlated. The characteristics of these RIA have been described in detail [15].

Modeling

Modeling of MTX and OH-MTX kinetics was performed according to the linear compartment models presented in Fig. 1. Two basic structures were considered. The first one (model I) corresponds to the classical model with elimination from the central compartment (No. 1). In the second structure (model II) it is assumed that MTX elimination (OH-MTX formation and other elimination pathways) occurs from a peripheral compartment (No. 2). In both cases, compartments 4 and 5 correspond to peripheral distribution compartments of MTX and OH-MTX respectively.

The model parameters were the following:

(i) the rate constants accounting for intercompartmental mass transfer (K_{12}, K_{21}, K_{14}, K_{41}, K_{35}, K_{53}) whose identifiability depends on the concentration-time profiles.

(ii) the rate constants for MTX elimination (OH-MTX formation and other elimination

Table 2. Pharmacokinetic parameters for MTX and OH-MTX

Patient		Cl ($l.h^{-1}$)	V_1 (l)	Kel_{MTX} (h^{-1})	K_{12} (h^{-1})	K_{21} (h^{-1})	K_{14} (h^{-1})	K_{41} (h^{-1})	$K_{13/V3}$ ($h^{-1}.l^{-1}$)	$Kel_{OH\text{-}MTX}$ (h^{-1})	K_{35} (h^{-1})	K_{53} (h^{-1})
1	TD	6.2	10.3	0.262	1.68	0.464	0.094	0.078	1.90×10^{-3}	0.053	—	—
	TD + FA	7.4	6.9	0.288	3.41	0.625	0.160	0.065	1.89×10^{-3}	0.047	—	—
2	TD + FA	12.1	14.3	0.365	1.79	0.407	0.053	0.067	1.39×10^{-3}	0.086	—	—
	TD	9.9	9.8	0.254	1.99	0.249	0.0042	0.024	1.43×10^{-3}	0.092	—	—
	HDI	5.4	9.7	0.513	4.69	3.81	0.0016	0.050	2.22×10^{-3}	0.102	0.036	0.020
3	TD	4.6	14.1	0.294	0.97	0.578	0.051	0.059	1.72×10^{-3}	0.084	—	—
	TD + FA	3.6	12.1	0.285	0.90	0.569	0.057	0.063	1.21×10^{-3}	0.067	—	—
	HDI	3.1	14.2	0.218	—	—	0.0071	0.033	4.35×10^{-4}	0.099	0.026	0.027
4	TD + FA	10.3	13.5	0.341	1.47	0.313	0.024	0.074	1.83×10^{-3}	0.074	—	—
	TD	10.9	11.4	0.518	1.75	0.426	0.038	0.070	1.62×10^{-3}	0.080	—	—
	HDI	4.3	2.3*	0.288	4.55*	0.409	0.014	0.044	7.77×10^{-4}	0.159	0.018	0.027
5	TD	14.0	14.6	0.331	2.12	0.400	0.059	0.107	1.31×10^{-3}	0.096	—	—
	TD + FA	11.6	17.3	0.261	2.15	0.574	0.032	0.023	1.47×10^{-3}	0.126	—	—
	HDI	6.1	19.3	0.314	—	—	0.0019	0.026	1.64×10^{-3}	0.064*	0.063*	3.53×10^{-3}*
6	TD	10.2	11.3	0.433	1.50	0.289	0.110	0.111	1.66×10^{-3}	0.090	—	—
	TD + FA	14.1	14.2	0.415	1.96	0.405	0.083	0.052	1.16×10^{-3}	0.082	—	—
	HDI	8.2	10.5	0.777	—	—	0.0025	0.038	2.39×10^{-3}	0.093	—	—
7	TD + FA	11.4	7.8	0.613	4.02	1.07	0.068	0.085	9.98×10^{-4}	0.125*	0.057*	8.25×10^{-3}
	TD	13.1	9.3	0.845	5.58	2.51	0.202	0.138	9.81×10^{-4}	0.126	—	—
	HDI	6.3	17.6	0.357	—	—	0.0036	0.060	2.21×10^{-3}	0.396	0.031	0.056
8	TD	6.1	15.3	0.318	1.82	1.14	0.112	0.099	2.83×10^{-3}	0.030	—	—
	HDI	5.0	26.7	0.188	—	—	0.0087	0.042	6.01×10^{-4}	0.055	0.058	0.066
Mean	TD	9.4	12.0	0.407	2.18	0.757	0.084	0.086	1.68×10^{-3}	0.081	—	—
± S.D.		(3.4)	(2.3)	(0.198)	(1.42)	(0.761)	(0.061)	(0.035)	(0.54×10^{-3})	(0.029)	—	—
	TD + FA	10.1	12.3	0.367	2.24	0.566	0.068	0.061	1.42×10^{-3}	0.080	—	—
		(3.5)	(3.7)	(0.121)	(1.10)	(0.249)	(0.045)	(0.020)	(0.34×10^{-3})	(0.026)	—	—
	HDI	5.5	16.3	0.379	—	—	0.0056	0.042	1.47×10^{-3}	0.151	0.034	0.039
		(1.6)	(6.3)	(0.204)	—	—	(0.0046)	(0.011)	(0.85×10^{-3})	(0.125)	(0.015)	(0.020)

*Parameters with high level of correlation disregarded from the mean.

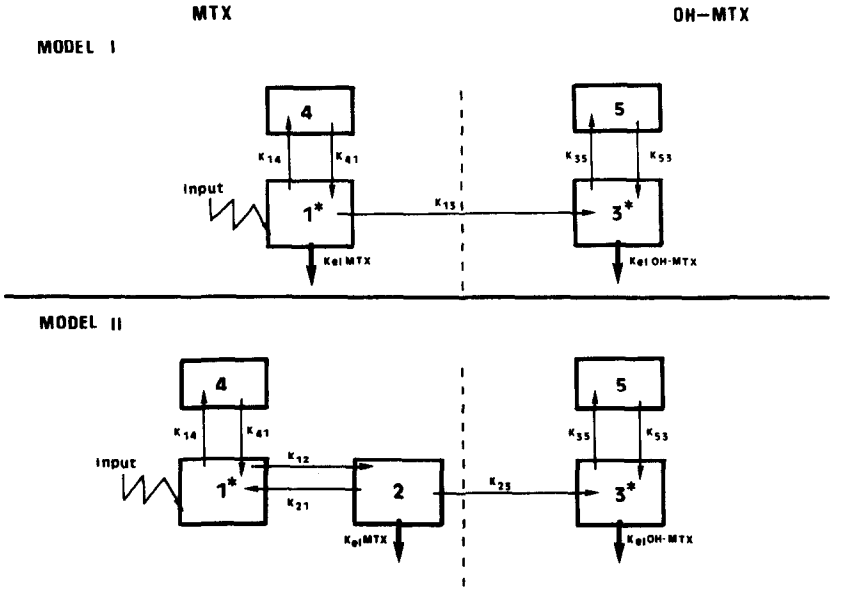

Fig. 1. Simultaneous modeling of MTX and OH-MTX disposition according to linear compartment models. Model I: MTX elimination (OH-MTX formation) from central compartment (No. 1). Model II: MTX elimination from a peripheral compartment (No. 2). (*) compartment sampled.

routes), K_{i3} and K_{i0}, respectively, where $i = 1$ for model I and $i = 2$ for model II, which are not identifiable separately. The estimated parameter is the overall elimination rate constant ($Kel_{MTX} = K_{i3} + K_{i0}$).

(iii) The OH-MTX elimination rate constant ($Kel_{OH\text{-}MTX}$).

(iv) the volumes of MTX and OH-MTX central compartments (V_1 and V_3, respectively). OH-MTX distribution volume (V_3) is not identifiable separately from the rate constant for OH-MTX formation (K_{i3}). The estimated parameter is thus the ratio K_{i3}/V_3.

These parameters made it possible to compute MTX total plasmatic clearance (Cl)

$Cl = Kel_{MTX} \cdot V_1$ in model I

$Cl = Kel_{MTX} \cdot V_1/(K_{21} + Kel_{MTX})$ in model II.

The choice of the model was dictated by its ability to fit the observed concentration–time profiles. Examination of the scatter of weighted residuals over time permitted evaluation of model validity.

The model was fitted to MTX and OH-MTX data simultaneously by using the SAAM program, which performs the integration of the set of differential equations describing the model [16]. A statistical weight was assigned at each data point, assuming an analytical variability with a constant coefficient of variation [17]. This was done because of assay conditions requiring serial dilutions of plasma samples [15].

Statistical analysis

Influence of FA administration of model parameters following intravenous administration was assessed by analysis of variance. Comparison of model parameters between TD and HDI was performed according to a paired *t*-test.

RESULTS

Figure 2 shows the fitting of model prediction on experimental data for a typical patient. Individual and mean parameter estimates are presented in Table 2.

Following intravenous bolus MTX administration (TD and TD-FA) model I could not simultaneously account for MTX and OH-MTX disposition kinetics and particularly, as indicated by the inspection of the plot of weighted residuals against time, it was not consistent with OH-MTX formation kinetics. Model II with OH-MTX formation occurring from a MTX peripheral compartment in rapid equilibrium with the central compartment as indicated by the high values of K_{12} and K_{21} adequately described both MTX and OH-MTX data following TD and TD-FA MTX administrations. Administration of FA was not of significant influence ($P > 0.05$) on both MTX and OH-MTX disposition parameters following intravenous bolus administration of MTX. For example, the mean ± S.D. estimation of Cl was 9.4 ± 3.4 and 10.1 ± 3.5 $l.h^{-1}$ following TD and TD-FA, respectively.

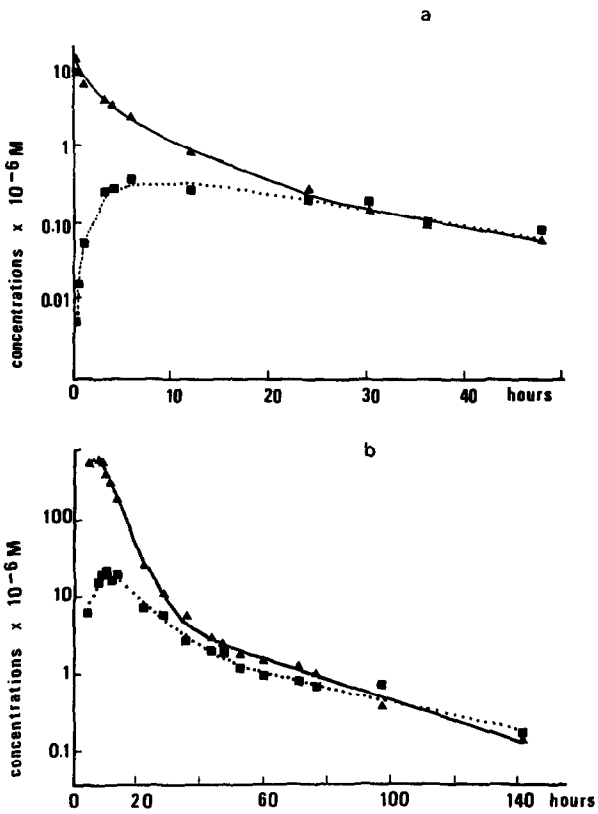

Fig. 2. Plasma concentration-time courses for MTX (▲) and OH-MTX (■) following intravenous bolus (TD-FA) and high-dose infusion (HDI) of MTX to patient No. 3. Solid and dotted lines represent the best fits of MTX and OH-MTX data, respectively.

Following HDI the data were consistent with model structure I in 5/7 cases. This is likely related to the differences in sampling protocol particularly during the early times of the profile (i.e. those characterizing OH-MTX formation kinetics). Also the distribution patterns of MTX and OH-MTX differed following HDI. Indeed the MTX peripheral distribution compartment (No. 4) identified was in slowest equilibrium with the central compartment as indicated by the 10-fold decreased value of K_{14} (Table 2). Moreover, a further distribution compartment (No. 5) was apparent on OH-MTX kinetic profile. This could be due to the higher doses administered and to the longer sampling time.

Following HDI a significant ($P < 0.01$) decrease of Cl was observed as compared with TD value (5.5 ± 1.6 vs. 9.4 ± 3.4 $l.h^{-1}$, respectively). However the parameters characterizing OH-MTX disposition remained unchanged, particularly those accounting for OH-MTX formation (K_{i3}/V_3) whose

mean value was of $1.47 \times 10^{-3} \pm 0.85 \times 10^{-3}$ and $1.68 \times 10^{-3} \pm 0.54 \times 10^{-3}$ $h^{-1}.l^{-1}$ following HDI and TD, respectively. OH-MTX elimination constant ($Kel_{OH\text{-}MTX}$) averaged 0.151 ± 0.125 h^{-1} following HDI and 0.081 ± 0.029 h^{-1} following TD.

DISCUSSION

The simultaneous modeling of MTX and OH-MTX data provides an integrated approach to assess the disposition of both compounds. This approach performs well in estimating the disposition parameters of a metabolite and particularly its elimination constant whatever the dosing protocol (intravenous bolus, infusion) and the disposition pattern. This would have not been possible using a model independent approach. Model I is the classical compartmental structure used in describing MTX pharmacokinetics [3–6, 12, 18–20]. Herein model II was justified as it accounts for OH-MTX kinetics.

Intravenous bolus (TD) of MTX were administered to estimate MTX clearance in order to individualize HDI [3, 6, 14]. The simultaneous administration of FA (TD-FA) had no influence on MTX nor on OH-MTX disposition kinetics. Consequently the identification of MTX pharmacokinetics following TD administration should allow for prediction of MTX levels not only during HDI [3, 5, 6] but also following HDI during FA rescue.

We showed in a retrospective study [6] the good performance of the TD protocol in predicting a wide range of infusion rates (17–650 mg/h) to achieve target MTX concentrations during various HDI protocols. However, we observed a trend to overestimate dosage requirements for very high rates of infusion (> 970 mgh). This would be due to the significant decrease of MTX plasmatic clearance between TD and HDI observed in this study. This might be explained by a saturation of an elimination process of MTX at such a high rate of delivery (> 1000 mg/h except for patient No. 8). Our present results indicate that the OH-MTX pathway is not responsible for this phenomenon which might instead be due to the renal clearance of MTX as previously reported [11, 21–25]. This is consistent with the results of Winograd *et al.* [26] who have demonstrated that renal clearance of MTX during the period of an infusion determines the overall body exposure to MTX. However this limitation of the TD protocol in predicting very high MTX infusion rates could be overcome by a feedback control of infusion rate using Bayesian estimation [19].

Acknowledgements—The authors are indebted to Mrs. J. Vigoux-Masse and the staff of the La Montagne unit (Institut Paoli-Calmettes, Marseille) for their collaboration, to Dr. A. Iliadis for helpful scientific suggestions, and to Drs D.G. Covell, J.N. Weinstein and J. Barbet for their help in using the SAAM program run on the Digital Equipment Corporation VAX 11-870 computer at the laboratory of Mathematical Biology of the National Cancer Institute (National Institutes of Health, Bethesda, MD) as well as for valuable discussions.

REFERENCES

1. Jolivet J, Cowan KH, Curt GA, Clendenin NJ, Chabner BA. The pharmacology and clinical use of methotrexate. *N Engl J Med* 1983, **309**, 1094–1104.
2. Reich SD. Mathematical modeling: guide to high-dose methotrexate infusion therapy. *Cancer Chemother Pharmacol* 1979, **3**, 25–31.
3. Monjanel S, Rigault JP, Cano JP, Carcassonne Y, Favre R. High-dose methotrexate: preliminary evaluation of a pharmacokinetic approach. *Cancer Chemother Pharmacol* 1979, **3**, 189–196.
4. Evans WE. Methotrexate. In: Evans WE, Schendag JJ, Jusko WJ eds. *Applied Phamacokinetics. Applied Therapeutics*. San Francisco, 1980.
5. Kerr IG, Jolivet J, Collins JM, Drake JC, Chabner BA. Test-dose for predicting high-dose methotrexate infusions. *Clin Pharmacol Ther* 1982, **33**, 44–51.
6. Cano JP, Bruno R, Lena N, Favre R, Iliadis A, Imbert AM. Dosage predictions in high-dose methotrexate infusions. Part 1: Evaluation of the classical test-dose protocol. *Cancer Drug Deliv* 1985, **2**, 271–276.
7. Goldman ID. The characteristics of the membrane transport of amethopterin and the naturally occuring folates. *Ann N Y Acad Sci* 1971, **186**, 400–422.
8. Lankelma J, van der Kleijn E. The role of 7-hydroxymethotrexate during methotrexate anticancer therpay. *Cancer Lett* 1980, **9**, 133–142.
9. Fabre G, Goldman ID. Formation of 7-hydroxy-methotrexate polyglutamyl derivatives and their cytotoxicity in human chronic myelogenous leukemia cells *in vitro*. *Cancer Res* 1985, **45**, 80–85.
10. Jacobs SA, Stoller RG, Chabner BA, Johns DG. 7-Hydroxymethotrexate as a urinary metabolite in human subjects and rhesus monkeys receiving high-dose methotrexate. *J Clin Invest* 1976, **57**, 534–538.
11. Jacobs SA, Stoller RG, Chabner BA, Johns DG. Dose-dependent metabolism of methotrexate in man and rhesus monkeys. *Cancer Treat Rep* 1977, **61**, 651–656.
12. Breithaupt H, Kuenzlen E. Pharmacokinetics of methotrexate and 7-hydroxymethotrexate following infusions of high-dose methotrexate. *Cancer Treat Rep* 1982, **66**, 1733–1741.

13. Fabre G, Cano JP, Iliadis A *et al.* Assay of methotrexate and 7-hydroxymethotrexate by gradient-elution high performance liquid chromatography and its application in a high-dose pharmacokinetic study. *J Pharm Biomed Anal* 1984, **2**, 61–72.
14. Favre R, Monjanel S, Alfonsi M *et al.* High-dose methotrexate: a clinical and pharmacokinetic evaluation. *Cancer Chemother Pharmacol* 1982, **9**, 156–160.
15. Bore P, Rahmani R, Cano JP, Just S, Barbet J. Radioimmunoassays of 7-hydroxymethotrexate and methotrexate. *Clin Chim Acta* 1984, **141**, 135–149.
16. Berman M, Weiss MF. *SAAM Manual.* DHEW publication No. (NIH) 78–180.
17. Peck CC, Beal SC, Sheiner LB *et al.* Extended least square nonlinear regression: a possible solution to the 'choice of weights' problem in analysis of individual pharmacokinetic data. *J Pharmacokin Biopharm* 1984, **12**, 545–558.
18. Stoller DG, Jacobs SA, Drake JC, Lutz RJ, Chabner BA. Pharmacokinetics of high-dose methotrexate (NSC-740). *Cancer Chemother Rep* Part 3, 1975, **6**, 19–24.
19. Iliadis A, Bachir-Raho M, Bruno R *et al.* Bayesian estimation and prediction of clearance in high-dose methotrexate infusions. *J Pharmacokin Biopharm* 1985, **13**, 101–115.
20. Bruno R, Iliadis A, Favre G, Lena N, Imbert AM, Cano JP. Dosage predictions in high-dose methotrexate infusions. Part 2: Bayesian estimation of methotrexate clearance. *Cancer Drug Deliv* 1985, **2**, 277–283.
21. Reich SD, Bachur NR, Goebel RH, Berman M. A pharmacokinetic model for high-dose methotrexate infusions in man. *J Pharmacokin Biopharm* 1977, **5**, 421–433.
22. Lawrence JR, Steele WH, Stuart JFB, McNeill CA, McVie JG, Whiting B. Dose dependent methotrexate elimination following bolus intravenous injection. *Eur J Clin Pharmacol* 1980, **17**, 371–374.
23. Hendel J, Nyfors A. Nonlinear renal elimination kinetics of methotrexate due to a saturation of renal tubular reabsorption. *Eur J Clin Pharmacol* 1984, **26**, 121–124.
24. Chen ML, Chiou WL. Pharmacokinetics of methotrexate and 7-hydroxymethotrexate in rabbits after intravenous administration. *J Pharmacokin Biopharm* 1983, **11**, 499–513.
25. Chen ML, Chiou WL. Clearance studies of methotrexate and 7-hydroxymethotrexate in rabbit after multiple-dose infusion. *J Pharmacokin Biopharm* 1983, **11**, 515–527.
26. Winograd B, Lippens RJJ, Oosterbaan MJM, Dirks MJM, Vree TB, van der Kleijn E. Renal excretion and pharmacokinetics of methotrexate and 7-hydroxy-methotrexate following a 24-h high dose infusion of methotrexate in children. *Eur J Clin Pharmacol* 1986, **30**, 231–238.